

Date of publication xxxx 00, 0000, date of current version xxxx 00, 0000.

Digital Object Identifier 10.1109/ACCESS.2023.0322000

# NeuroAssist: Open-Source Automatic Event Detection in Scalp EEG

MOHAMMAD ALI ALQARNI<sup>1</sup>, HIRA MASOOD<sup>2</sup>, ADIL JOWAD QURESHI<sup>2</sup>, MUIZ ALVI<sup>2</sup>, HAZIQ ARBAB<sup>2</sup>, HASSAN AQEEL KHAN<sup>3, 1</sup>, AWAIS MEHMOOD KAMBOH<sup>1, 2</sup>, SAIMA SHAFAIT<sup>4</sup>, FAISAL SHAFAIT<sup>2, 5</sup>

<sup>1</sup>College of Computer Science and Engineering, University of Jeddah, Jeddah, Saudi Arabia

<sup>2</sup>School of Electrical Engineering and Computer Science, National University of Sciences and Technology, Islamabad, Pakistan

<sup>3</sup>Department of Applied Artificial Intelligence and Robotics, School of Computer Science and Digital Technologies, Aston University, Birmingham, B4 7ET, UK

<sup>4</sup>Pak-Emirates Military Hospital, Rawalpindi, Pakistan

<sup>5</sup>Deep Learning Laboratory, National Center of Artificial Intelligence, Islamabad, Pakistan

Corresponding author: Hassan Aqeel Khan (e-mail: h.khan54@aston.ac.uk)

**ABSTRACT** Localisation of clinically relevant events within Electroencephalogram (EEG) recordings can be useful for explaining the decisions made by automated EEG screening and decision support systems. The majority of existing deep learning based approaches that have been proposed in recent literature only classify EEG records as normal or pathological without providing any justification for their decisions and thus are not very transparent. In clinical practice it is often observed that a significant proportion of EEG recordings does not contain any abnormal (or pathological) events; even in cases classified as pathological. If deployed in practice such a setup would not be very useful since it would require neurologists to invest additional time, manually searching for events within an EEG recording before accepting or rejecting the decision proposed by the automated system. This work presents open-source software that can automatically localise and classify abnormalities both across time and EEG channels. Our work can thus be used to reveal the reasons behind an EEG recording being classified as normal or pathological/abnormal. Training an automated event localisation system requires a dataset containing fine-grained labels pointing out precise locations of events. To facilitate further development we are also releasing the dataset and annotations used in this work for use by the research community. This dataset contains 1,075 EEG recordings with precise temporal and channel locations of two broad categories of abnormal events: (i) Epileptiform discharges and (ii) Non-epileptiform abnormalities. Our localisation system is based on features derived from wavelet transforms. For event classification we investigated the performance of both classic machine learning algorithms (support vector machines, decision trees, random forest classifier) and deep convolutional neural networks (VGG16, GoogLeNet and EfficientNet). Our results indicate that deep convolutional neural networks outperform classic machine learning algorithms in terms of average values of precision, recall, F1-score and accuracy.

**INDEX TERMS** Abnormality localisation, Automated EEG analysis, Computer aided diagnosis, Computational neurology, Convolutional neural networks, Deep learning, Open-source EEG dataset.

## I. INTRODUCTION

**A**N electroencephalogram (EEG) is a painless test that allows us to acquire electrical activity of the brain using sensors mounted on the scalp. EEGs have been in use since the 1930s [3] and are cheaper to maintain and administer compared to other NeuroImaging tools such as MRIs and CT scans. Lower costs and wide availability make EEGs appealing tools for provision of neurological care in the resource-constrained healthcare systems of developing countries. However, low hardware cost is not the only factor

obstructing quality neurological care in under-served areas. Another, perhaps more serious, challenge is the scarcity of qualified neurologists who can interpret EEGs and devise treatment plans based on them. According to the WHO, the total neurological workforce (which includes neurologists, neurosurgeons and child neurologists) in high-income countries stands at a median value of 7.3 per 100,000 population [4]. In developing countries, by contrast, this drops to a mere 0.1 per 100,000 population.

Telehealth systems can ameliorate the situation in under-

served areas by connecting neurologists with patients in virtual clinics; however, given the acute shortage of doctors, simple telehealth systems can reach full-capacity fairly quickly. Smart solutions that leverage Artificial Intelligence (AI) and Machine Learning (ML) to introduce efficiency and intelligence into the telehealth pipeline are thus more likely to be adopted in practice. In the domain of tele-neurology an AI-enabled EEG system could be used for the following purposes:

- (1) Screen pathological/abnormal EEG records and forward them to neurologists for further analysis.
- (2) Highlight regions that may be of interest to the neurologists for diagnosis or analysis.
- (3) Provide explanations and statistics that allow neurologists to promptly analyze EEG recordings.
- (4) Automatically quantify and archive records that may be useful for research later.

In the preceding list, theme-1 has been explored in prior literature [5]–[8]. **This paper is focused on theme-2**, while theme-3 and theme-4 are left for future work. Training learning algorithms to detect events of interest requires annotations indicating event locations, consequently, we had to invest considerable effort in generating fine-grained labels for events within EEG recordings. This labelled dataset was used to train learning algorithms to localise EEG events of interest (EOIs). Event localisation has numerous benefits, the primary being the ability to promptly interpret why an EEG record is classified as normal or pathological/abnormal. Consequently, this capability can be used to lay the foundation of a system that can incorporate transparency and explainability within EEG based decision support systems (theme-3). Furthermore, event localisation can also be useful for quantification and archiving systems that can promptly process large volumes of EEG data (theme-4). In this work, we focus primarily on localisation of two types of abnormal waveforms (1) Epileptiform discharges ( i.e. spike, polyspike, and sharp waves) (2) Non-epileptiform abnormalities ( i.e. slow waves ). These EEG patterns are representative of abnormal electrocerebral activity. Spike and sharp waves are considered diagnostic of epilepsy in appropriate clinical settings; slow waves (either focal or generalised) can also be indicative of underlying cerebral dysfunction. These non-epileptiform abnormalities, independently or sometimes intermixed with epileptiform discharges, are seen in a multitude of neurological disorders e.g. in cerebral hypoxia, encephalopathy, infections, and degenerative brain disorders.

The current landscape of automated EEG analysis systems reveals several critical gaps that this research aims to address. One significant gap is the lack of transparency in existing deep learning-based approaches, which in most cases provide only a binary classification decision [31] [32]. Despite the advancements in deep learning techniques for EEG screening [33], there remains a pressing need for greater interpretability and explainability in these models. This research aims to bridge these gaps by developing more transparent and inter-

pretable models for EEG analysis. Given that the duration of clinical EEG recordings can extend up to hours, a simple screening system would require a neurologist to perform a detailed scan of the recording before preparing a report or diagnosis. After screening, our system can be used to localise and highlight relevant events (across both time and EEG channels) enabling prompt EEG quantification, and therefore, can be a valuable analysis tool for neurologists.

One reason why there aren't many existing EEG event localisation systems is the scarcity of detailed, labeled, datasets necessary for training and validating them. Labeling EEG data with precise annotations is a labor-intensive process that requires expert knowledge, leading to a limited number of available datasets. Our contribution includes the creation and public release of a comprehensive dataset containing 1,075 EEG recordings with fine-grained labels indicating the precise temporal and channel locations of two broad categories of abnormal events: epileptiform discharges and non-epileptiform abnormalities. By making this dataset available to the research community, we aim to facilitate further advancements in the field of automated EEG analysis.

Given the sparsity of existing literature on event localisation, a thorough performance evaluation of the different types of learning algorithms is also required. When it comes to performance, the default assumption made by most researchers is that deep convolutional neural networks (DCNNs) will outperform classical machine learning (CML) algorithms. Given the novelty of our dataset, we have not made this assumption and have opted for an evidence based approach to examine the performance difference between DCCNs and CML algorithms, such as support vector machines (SVMs), decision trees, and random forest classifiers. Furthermore, CML algorithms are easier to interpret and train compared to DCCNs and should not be dismissed without compelling evidence to demonstrate a substantial performance gap compared to DCNNs. Another area requiring further investigation is identifying suitable features for the event localisation application. We examine the performance of a number of different wavelet based features, in conjunction with different learning algorithms, to examine which set of features works best. We focus on features derived from the wavelet transform because wavelets can easily capture subtle variations in EEG signals [30].

The **salient contributions** of this work are listed below:

- Significant effort has been invested in creating a large, labelled dataset of EEG records with event locations across both time and channels. The detailed event annotations in this dataset should be very useful for researchers interested in investigating interpretability and explainability in the context of EEG. This dataset, called NMT-Events, is being released publicly under the Creative Commons by Attribution licence (CC BY <sup>1</sup>) and is

<sup>1</sup>Access creative commons by Attribution Licence: <https://creativecommons.org/licenses/by/4.0/>

available for download <sup>2</sup>.

- Our dataset is the only publicly available EEG dataset containing detailed event level annotations that has been collected from a South Asian demographic.
- Performance of DCNN and conventional machine learning algorithms is compared on the task of EEG event localisation.
- Performance is evaluated for wavelet based feature extraction on the event localisation problem using 6 different learning algorithms.
- For the purpose of result replication and benchmarking, all the code used for the experiments in this paper is being released publicly: <https://github.com/dll-ncai/Localization-of-Abnormalities-in-EEG-Waveforms.git>

By addressing these research gaps, our work not only advances the field of automated EEG analysis but also provides valuable tools and datasets that can be used by other researchers to further develop and refine AI-based diagnostic systems.

## II. RELATED WORK

The task of automatic event localization in EEG records is challenging due to the extensive effort required for labeling individual events, leading to a limited number of studies addressing this issue. One notable attempt is [10], where six different event types were detected using mel-frequency cepstral coefficients (MFCC). While MFCCs are widely used in speech recognition, their application in EEG analysis is debatable. The authors of [10] utilized a variant called linear frequency cepstral coefficients (LFCC) for EEG data. However, the generalizability of speech recognition features to EEG remains questionable. In contrast, deep convolutional neural networks (DCNNs), which are designed for imaging applications, might be more suitable for extracting image-based features from EEG data. Our approach involves converting EEG signals into images using wavelet transforms to capture the time-frequency variations effectively.

Traditional machine learning algorithms such as support vector machines (SVMs), decision trees, and random forest classifiers have also been used in EEG classification tasks. SVMs, noted for their efficacy in high-dimensional spaces, have been successfully applied to EEG data as demonstrated in [25]. Decision trees provide simplicity and interpretability, making them useful for initial EEG classification models, as noted in [26]. Random forest classifiers, being ensembles of decision trees, enhance accuracy and robustness by mitigating overfitting, as shown in [27].

In the realm of deep learning, various architectures have been explored for EEG analysis. For example, [28] reviews the effectiveness of convolutional neural networks (CNNs) such as VGG16, GoogLeNet, and EfficientNet in EEG-based applications, including emotion recognition and sleep stage scoring. These architectures have shown significant improve-

ments in processing and interpreting complex EEG data, highlighting their potential in advancing automated EEG analysis.

Deep learning has also been applied to the detection of epileptic events, achieving a reported accuracy of 99% in [11]. However, the dataset in this study was small, consisting of only 500 EEG segments, each 23.6 seconds long. This limited dataset likely means that performance will degrade in real-world settings. In contrast, our dataset is collected in a hospital environment, with significantly longer EEG recordings averaging approximately 20 minutes.

Most existing literature on localization focuses on detecting the onset of specific disorders or pathologies within an EEG recording. For example, seizure onset has been examined in [12] and [13]. EEG is also crucial for sleep pattern analysis and diagnosing sleep disorders, with sleep-related micro-events localized using deep learning in [14]. Our approach differs by focusing on generic events of interest in EEG pathology rather than specific disorders and therefore has the potential to be applied in a broad range of problems.

In summary, while existing literature provides a foundation for EEG event localization, our work advances these efforts by targeting a broader range of abnormal events and leveraging advanced deep learning techniques to improve accuracy and interpretability.

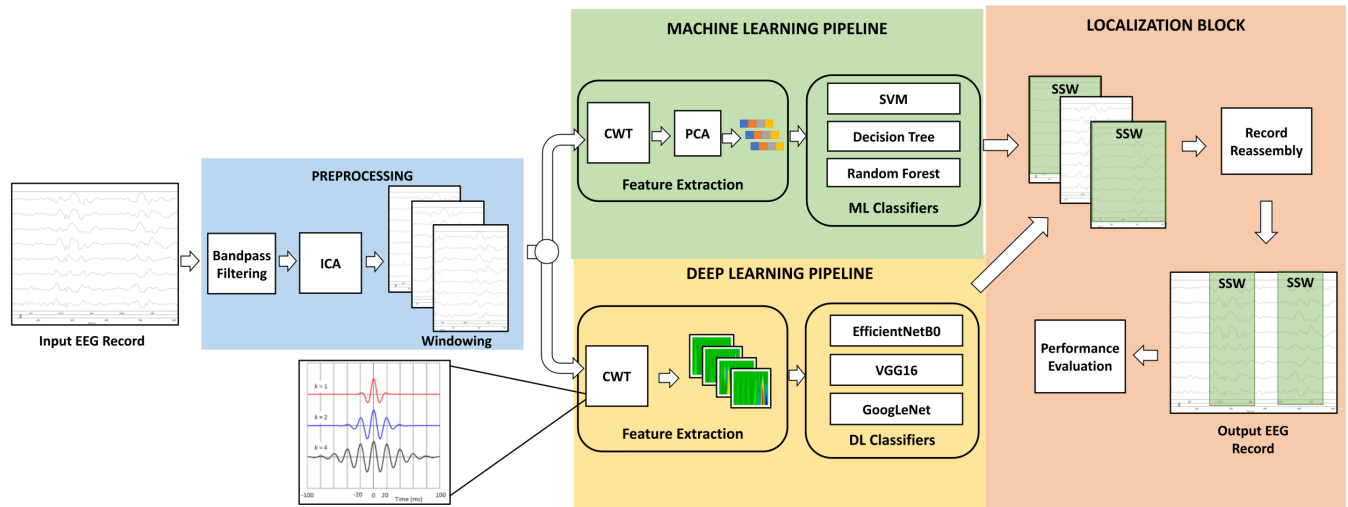
## III. MATERIALS AND METHODS

Figure 1 provides an overview of the approach used for event localisation; the process begins by segmenting each input record into 2-second windows, with a 50% overlap between consecutive windows. Given that our EEG data is sampled at a frequency of 200 Hz, each window contains 400 data samples.

We explore two distinct learning pipelines to evaluate the performance of both traditional machine learning algorithms and contemporary deep learning algorithms. The machine learning pipeline investigates three CML classifiers: support vector machines (SVMs), decision trees, and random forest classifiers. These classifiers are chosen for their robustness and widespread use in various classification tasks. In contrast, the deep learning pipeline examines three DCNN models: VGG16 [19], EfficientNetB1 [21], and GoogLeNet [20]. These models are selected for their proven effectiveness in image classification tasks and their varying architectural complexities.

To prepare the data for both pipelines, we generate image-based feature vectors by applying the Continuous Wavelet Transform (CWT) [9] to the segmented data windows. This transformation converts the time-domain EEG data into a time-frequency representation, which is more suitable for analysis by both machine learning classifiers and DCNN models. Finally, the performance of each model is evaluated by comparing their predictions to the ground truth labels in the dataset. This comparison allows us to assess the accuracy and effectiveness of both the traditional machine learning classifiers and the deep learning models in processing and interpreting EEG data.

<sup>2</sup>Download creative commons by Attribution Licence: <https://1drv.ms/f/s!AIVxrt288kY0g8Uc5Aa36axB62Gv8w?e=k0PCvr>



**FIGURE 1.** High level overview of our approach. An input EEG record is first broken down into small sized windows. The wavelet transform is used to extract features from each window. A classifier uses the wavelet features to assign an event label to each window. Window locations are then mapped back to obtain predictions of events in the input record.

**A. DATASET**

Data collection for this research was done at the Pak-Military hospital (MH) in Rawalpindi, Pakistan. Our study was approved by the hospital’s Institutional Review Board (IRB)<sup>3</sup>. Data was collected after obtaining informed consent from all participants involved in this study. The hardware used for data acquisition was KT88-2400 developed by Contec Medical Systems. All participants were advised to not take any kind of sleep medication or sedative for at least one day before the recording session. The recording sessions were conducted by a qualified technician with over 6 years of experience in EEG recording. Each participant’s data was subsequently labeled by a team of neurologists at the hospital. The labeling process involved reviewing the entire record and marking the start and stop times, as well as channel instances of events of interest. The labels were stored in a Comma Separated Values (CSV) file using an open-source tool developed specifically for the NeuroAssist project. To ensure high inter-scorer reliability, the labeled data was then verified by two expert neurologists who either approved or corrected any misclassifications identified by the initial labeling team.

Participants were asked to lie comfortably and keep their eyes open. They were instructed to minimize movement and blinking to reduce artifacts. This condition helps capture EEG patterns associated with active visual processing and alertness. Participants were then asked to close their eyes and relax while remaining awake. This condition is useful for capturing resting-state EEG activity, characterized by prominent alpha rhythms, particularly in the occipital region.

The EEG data was acquired at a sampling rate of 200 Hz using a standard 10/20 setup, encompassing 21 channels with A1 and A2 as standard reference channels. All EEG records were stored in the European Data Format (EDF). The

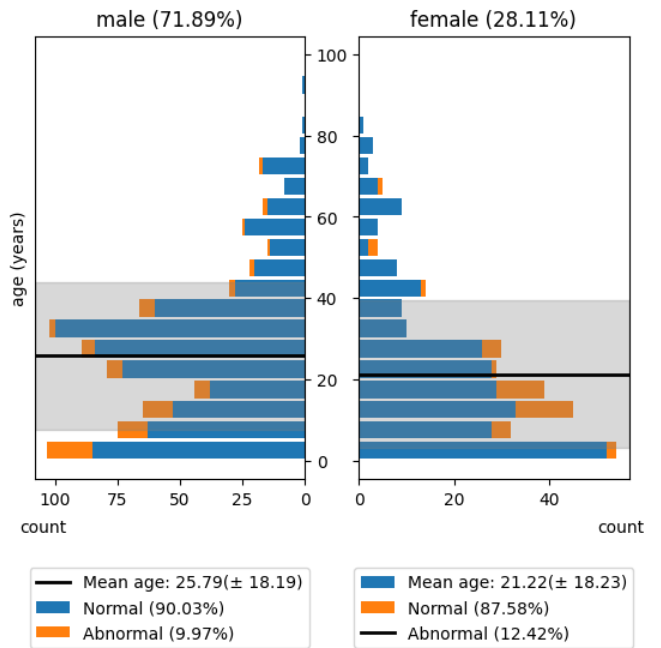


**FIGURE 2.** Demographics of the NMT-Events dataset, segregated by gender, age, and class label.

dataset comprises a total of 1,075 records, with 113 records showing abnormalities and 962 records being normal. The dataset demographics indicate that approximately 71.63% of the recordings were collected from male participants, while 28.37% were from female participants, with participant ages ranging from 6 to 93 years. We have removed EEG recordings of participants younger than 6 years old from our dataset. This decision was made to avoid the substantial developmental changes in EEG patterns that occur during early childhood. These differences can complicate the analysis and interpre-

<sup>3</sup>IRB number: MH51214 (Dated March-15-2019)

**TABLE 1. Classification of EEG abnormalities into corresponding super classes.**

Class	Super Class
Spike and Wave	SSW
Spikes	SSW
Polyspikes	SSW
Polyspikes and Wave	SSW
Sharp Wave	SSW
Sharp and Slow Wave	SW
Delta Slow Wave	SW
Sharp and Delta Slow Wave	SW

tation of EEG data when comparing across a broader age range. By focusing on participants older than 6 years, the study might aim to minimize variability introduced by developmental changes in brain activity, thereby ensuring more consistent and reliable results.

Figure 2 illustrates the demographics of the dataset, segmented by gender, age, and class label. The mean age for male participants was 25.58 years ( $\pm 18.33$ ), with 90.26% of the male recordings being normal and 9.74% abnormal. For female participants, the mean age was 21.15 years ( $\pm 18.12$ ), with 88.03% of the recordings being normal and 11.97% abnormal.

Overall, nine different categories of events have been labeled in the NMT-Events dataset. For the purpose of this work, these nine events were merged into two broad super classes: ‘Slow Waves’ (SW) and ‘Spike and Sharp Waves’ (SSW) according to the grouping shown in Table 1. For instance, ‘Polyspikes’ were included in the ‘Spike and Sharp Waves’ category due to their nature as repeated occurrences of spike and wave abnormalities. Similarly, all slow waves, including ‘Delta Slow’ and ‘Sharp and Slow Waves,’ were categorized under ‘Slow Waves’. This classification was based on their significance in clinical diagnosis, as confirmed by certified neurologists. Furthermore, it is emphasized that although the labels of these nine event categories are not used in this work, they are available in the dataset for researchers interested in using them. This dataset is one of the few publicly available EEG datasets collected from a South Asian demographic, providing valuable data for further research and analysis.

## B. PRE-PROCESSING

During the pre-processing stage, several essential steps were implemented to prepare the data for analysis. Initially, the data was filtered using a Hamming window-based bandpass filter with a lower passband edge at 1.00 Hz and an upper passband edge at 45.00 Hz. This filter featured -6 dB cutoff frequencies at 0.50 Hz and 50.62 Hz, to effectively eliminate electrical noise, particularly the 60 Hz interference potentially introduced by the hardware. Subsequently, Independent Component Analysis (ICA) was employed to decompose the

**TABLE 2. Dataset Partitions and Label Distribution: This table presents the partitioning of the dataset into training, validation, and testing sets, along with the distribution of window labels for each set. The labels include Normal, Slow Waves (SW), and Spike and Sharp Waves (SSW) conditions.**

Dataset Partition	Number of Recordings	Label Distribution		
		Normal	SW	SSW
Train	726	149,025	94,965	63,085
Valid	135	25,540	16,758	11,132
Test	214	41,882	22,806	22,371

multivariate EEG signals into independent components. This process targeted the removal of muscle artifacts, such as those originating from jaw clenching or facial muscle movements, thereby preserving the underlying brain signals for further analysis.

For event localization, each record was divided into 2-second windows with a 50% overlap between successive windows. Each window was assigned one of the three event labels based on the label file provided by the neurologists. The use of a small window size was intentional to achieve high temporal resolution. However, windowing results in discretization since windows at the edges of events might not fully contain an event. To address this, a discretization threshold of 25% was employed; a window with an overlap of 25% or more with an event (SW or SSW) was labeled as an event window and was assumed to contain the event in its entire span. During the output stage, each 2-second window was assigned a predicted class label, and these labels were combined to obtain event labels for the entire, uncropped EEG record.

Given the inherently unbalanced nature of the dataset, where normal events significantly outnumber abnormal events, balancing was introduced to avoid introducing bias into the classifiers. More specifically, we selected a random subset of normal windows to approximately match the total number of abnormal windows (including both SW and SSW). The process of selecting normal windows consisted of two main steps: i) selecting random normal windows from completely normal records, and ii) choosing fully normal windows from abnormal records. The dataset was partitioned into three subsets: training, validation, and test, using a ‘*subject-based division*’ rather than random selection. This means that data windows from a single subject/participant were assigned exclusively to only one of the three (training, validation, or test) sets, this was done to prevent data leakage between the sets. The size of the partition sets and event/label distribution can be seen in Table 2.

## C. FEATURE EXTRACTION

Although a large number of options are available for feature extraction from EEG data, we decided to employ features based on wavelet transforms which are extremely useful tools for time-frequency analysis of natural signals. Additionally, their multi-resolution characteristics enable effective localisation of events in non-stationary signals making them quite ap-

peeling for our target application. There are two main flavours of the wavelet transform: the Discrete Wavelet Transform (DWT) and the Continuous Wavelet Transform (CWT). The DWT decomposes signals into approximation and detail coefficients via filtering and downsampling, whereas the CWT operates on a continuous scale. Our study focuses on the CWT due to its superior ability to capture the visual characteristics of signal events. Furthermore, in our preliminary analysis the DWT did not yield satisfactory performance for detecting signal events leading us to abandon further investigation.

The CWT involves convolving a signal  $x(t)$  with scaled and shifted versions of a mother wavelet  $\psi(t)$ . We conducted an extensive comparison of multiple mother wavelets to evaluate their effectiveness in capturing various signal characteristics. The wavelets assessed include the Morlet wavelet, Mexican Hat wavelet, Gaussian 1st Derivative wavelet, and Gaussian 2nd Derivative wavelet, each offering unique properties for signal analysis.

### 1) Morlet Wavelet

The Morlet wavelet combines sinusoidal oscillation with a Gaussian envelope, effectively capturing both frequency and temporal aspects [22]. It is defined as follows:

$$\psi(t) = C_\sigma \pi^{-0.25} e^{-0.5t^2} (e^{j\sigma t} - K_\sigma) \quad (1)$$

where,

- $t$  denotes the time variable.
- $j$  represents the imaginary unit (i.e.,  $j^2 = -1$ ).
- $\sigma$  is a parameter that controls the oscillation of the wavelet.
- $C_\sigma$  and  $K_\sigma$  are scaling parameters derived from  $\sigma$ .

The Gaussian envelope term  $e^{-0.5t^2}$  ensures that the wavelet has good time localization, decaying rapidly as  $t$  moves away from zero. The sinusoidal term  $e^{j\sigma t}$  represents a complex sinusoidal function, where the parameter  $\sigma$  controls the frequency of oscillation. The correction factor  $K_\sigma$  ensures the wavelet has zero mean, necessary for analysis. Specifically,

$$C_\sigma = \left(1 + e^{-\sigma^2} - 2e^{-0.75\sigma^2}\right)^{-0.5} \quad (2)$$

$$K_\sigma = e^{-0.5\sigma^2} \quad (3)$$

### 2) Mexican Hat Wavelet (Ricker Wavelet)

The Mexican Hat wavelet, or Ricker wavelet, is characterized by its zero mean and compact support, making it particularly effective for detecting sharp signal changes [23]. It is defined as follows:

$$\psi(t) = (1 - t^2)e^{-t^2/2} \quad (4)$$

### 3) Gaussian Derivative Wavelets

The Gaussian 1st and 2nd Derivative wavelets are useful for capturing local variations and edges, detecting abrupt changes and fine details in signals [24]. The 1st Derivative Gaussian wavelet is defined as:

$$\psi'(t) = -te^{-t^2/2} \quad (5)$$

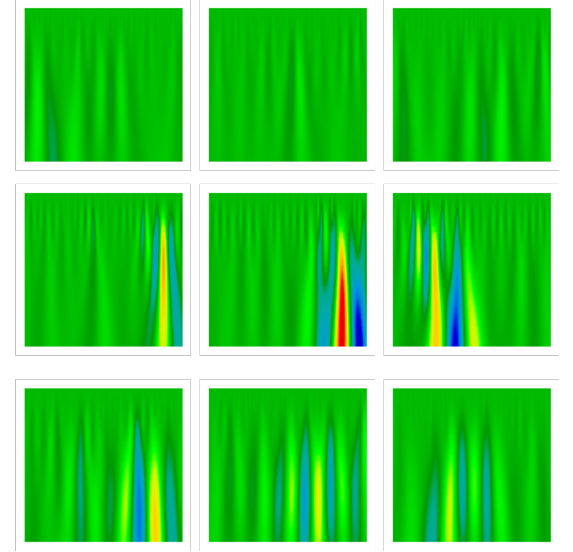


**FIGURE 3.** Scalograms of three randomly selected samples of all three events. The top row contains scalograms of three normal event windows. The middle and bottom rows contain three SSW and three SW event windows respectively.

The 2nd Derivative Gaussian wavelet is defined as:

$$\psi''(t) = (t^2 - 1)e^{-t^2/2} \quad (6)$$

The output of the CWT, known as a scalogram, provides a visual representation of a signal's characteristics in the time-frequency domain. The CWT for each EEG segment, was resized to 224x224 pixels to maintain consistency with the input requirements of our deep learning models. This resulted in a three-dimensional input tensor of shape (224, 224, 3), where the three channels correspond to different scales of the wavelet transform. Using 3 scales strikes a balance between capturing the necessary signal details and maintaining computational efficiency. Our preliminary experiments indicated that increasing the number of scales beyond 3 did not lead to significant performance improvements. In Figure 3 some examples of scalograms illustrate the similarities among event windows of the same category and the dissimilarities between different events. This ability to capture visual characteristics makes scalogram representations of EEGs suitable as input features for our deep learning pipeline. The CWT of a signal  $x(t)$  is expressed as:

$$X_{cwt}(a, b) = \int_{-\infty}^{\infty} x(t)\psi_{a,b}^*(t) dt \quad (7)$$

where  $\psi_{a,b}^*(t)$  denotes the complex conjugate of a scaled and shifted version of the mother wavelet  $\psi(t)$ ,  $a$  is the scaling parameter, and  $b$  is the shifting parameter. We utilized all the aforementioned mother wavelets in our study to capture a wide array of signal characteristics. Given the efficacy of scalograms in capturing the visual characteristics of events of interest, we utilized them as input features for both our deep learning and machine learning pipelines.

## D. MACHINE LEARNING ALGORITHMS

To tackle the challenges inherent in EEG event localization, our study's machine learning pipeline, illustrated in Figure 1, incorporates three prominent machine learning algorithms. Each algorithm is specifically chosen for its robust capabilities in processing complex data structures and patterns, particularly those involving intricate temporal and spatial dimensions. The selected algorithms are: Support Vector Machines (SVMs) [16], Decision Trees (DT) [18], and Random Forest (RF) [17] classifiers. Our goal is to develop a comprehensive understanding of the temporal dynamics within these brief intervals, which are critical for accurate localization of neurological events.

### 1) Support Vector Machines (SVMs)

SVMs are known for their ability to analyze high-dimensional data effectively. They achieve this by transforming the EEG signals into a higher-dimensional space using a kernel function. This characteristic is crucial for the 2-second EEG segments, which may contain intricate patterns related to specific neurological states that are difficult to discern in lower-dimensional spaces. In this study, SVM classifiers were employed with a linear kernel (`kernel='linear'`) to model the relationship between features and target labels within the EEG data. The linear kernel was selected for its simplicity and efficiency in high-dimensional spaces, where it can often perform comparably to more complex kernels, particularly when the data is well-separated [29]. To handle the non-linearity of EEG data, feature scaling was applied to the training and testing datasets. Initially, the features were standardized using `StandardScaler`, followed by normalization using `MinMaxScaler`. This two-step scaling process was crucial for ensuring that the features were on a comparable scale, thereby enhancing the performance of the SVM. The SVM classifier was configured with a regularization parameter `C=2.0`, which controls the trade-off between achieving a low error on the training data and maintaining a low model complexity. A higher `C` value was chosen to emphasize correct classification of the training data, even at the cost of allowing a smaller margin. The `decision_function_shape='ovr'` setting was used to enable a one-vs-rest strategy, where a binary classifier is trained for each class, making the approach suitable for multi-class EEG classification tasks. The `gamma='auto'` parameter allowed the model to automatically determine the influence of each training example, ensuring that the classifier could handle the variability in EEG data effectively. A fixed random state (`random_state=0`) ensured the reproducibility of the results. The classifier was trained separately for each wavelet-transformed version of the EEG data, allowing for the exploration of different frequency bands and their impact on classification accuracy. The model's performance was assessed using the transformed and scaled test data, providing insights into its ability to generalize across different EEG segments.

### 2) Decision Trees

Decision Trees are utilized for their straightforward, rule-based approach to classification and regression. They simplify the decision-making process by breaking down the dataset into smaller subsets and sequentially analyzing the impact of individual features. This method is particularly effective for short EEG segments, where rapid classification of neural events is necessary. Decision Trees offer clear visualization and interpretability of the decision paths, which is invaluable for debugging and refining the model based on specific EEG features that influence the outcome. For short segments like the 2-second slices of EEG data, Decision Trees can effectively handle the temporal dynamics and offer insights into which features most significantly impact the classification or localization task [18]. In this implementation, the Decision Tree classifier was configured using the entropy criterion for measuring the quality of splits. This criterion, based on information gain, is particularly useful for EEG data as it prioritizes features that reduce uncertainty in the classification task. The model was further optimized by setting `max_features=sqrt`, which limits the number of features considered at each split to the square root of the total number of features. This setting helps in reducing overfitting, ensuring that the model remains robust even when dealing with high-dimensional EEG data. The depth of the tree was constrained to a maximum of 5 (`max_depth=5`), balancing the need for model complexity with the risk of overfitting. This depth was chosen to ensure that the model could capture essential patterns in the EEG data without becoming overly complex. Additionally, the minimum number of samples required to be at a leaf node was set to 1 (`min_samples_leaf=1`), allowing the model to capture fine-grained distinctions in the data, which is important for detecting subtle neural events. The `splitter='best'` parameter was used to ensure that the most discriminative feature was chosen at each node, maximizing the effectiveness of each split. A fixed random state (`random_state=0`) was applied to ensure reproducibility of the results. Each Decision Tree model was trained separately on different wavelet-transformed versions of the EEG data, allowing the model to adapt to different frequency components and their relevance to the classification task.

### 3) Random Forest (RF) Classifiers

Building on the foundation of Decision Trees, RF classifiers employ an ensemble of trees to enhance predictive accuracy and robustness. This approach is crucial for dealing with the inherent variability and potential noise in EEG data [17]. By aggregating predictions from multiple decision trees, each constructed with a random subset of the data and features, Random Forests mitigate the over-fitting risk associated with single Decision Trees and improve generalization over diverse neurological conditions captured in short EEG segments. In this study, the Random Forest classifier was configured with specific hyperparameters to optimize its performance on EEG data. Specifically, the classifier was trained

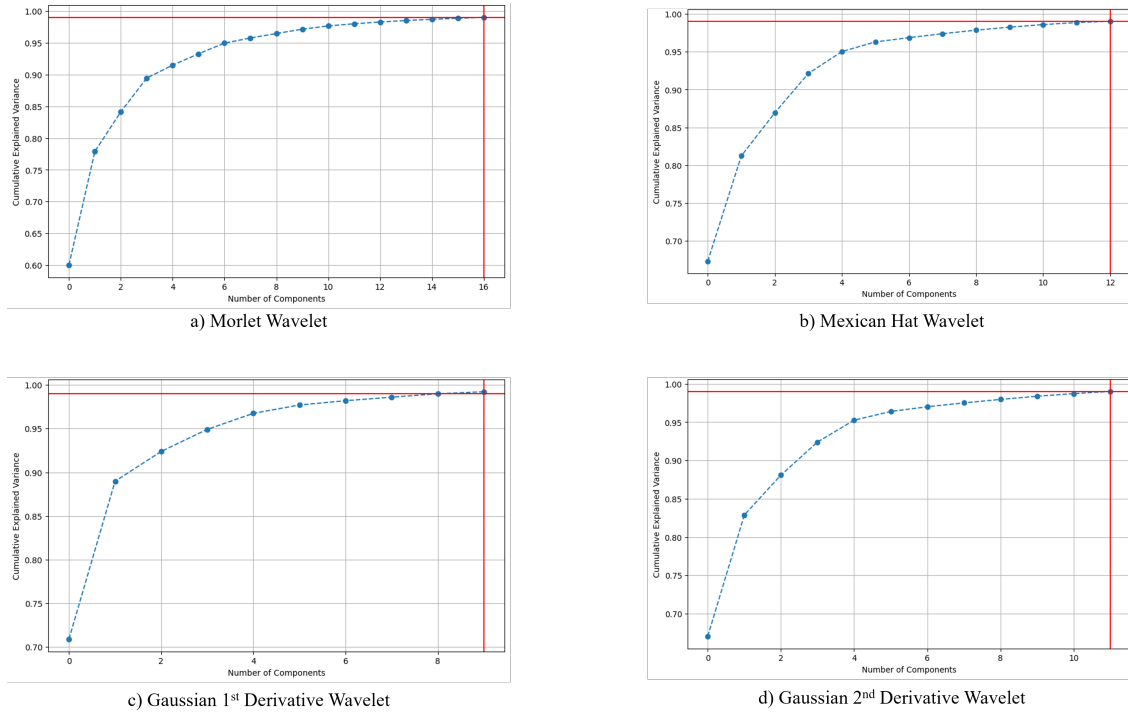


**FIGURE 4. Cumulative Explained Variance by Number of Principal Components.** Each graph shows the cumulative explained variance for different wavelet transforms used in EEG signal analysis. The red vertical lines indicate the number of principal components needed to capture 99% of the variance, with Morlet requiring 16, Mexican Hat 12, Gaussian 1<sup>st</sup> Derivative 9, and Gaussian 2<sup>nd</sup> Derivative 11 components.

using 100 decision trees ( $n\_estimators=100$ ), with the entropy criterion employed for measuring the quality of splits. The maximum number of features considered for each split was set to the square root of the total number of features ( $max\_features=sqrt$ ), which helps in maintaining diversity among the trees and enhances the robustness of the model. Furthermore, the depth of each tree was limited to 7 ( $max\_depth=7$ ), preventing the model from becoming overly complex and reducing the risk of overfitting. The minimum number of samples required to be at a leaf node was set to 2 ( $min\_samples\_leaf=2$ ), ensuring that each split is based on a sufficient amount of data. A fixed random state ( $random\_state=0$ ) was used to ensure reproducibility of the results. The classifier was trained on multiple wavelet-transformed versions of the EEG data, allowing for the exploration of different frequency bands and their contributions to the classification task. The performance of each trained Random Forest model was evaluated on a test dataset, and the results were analyzed to determine the classifier's ability to generalize across different EEG segments. This careful tuning of hyperparameters was essential in achieving reliable and interpretable classification outcomes in the context of automatic event detection in scalp EEG data. The performance of each trained Random Forest model was evaluated on a test dataset, and the results were analyzed to determine the classifier's ability to generalize across different EEG segments. This careful tuning of hyperparameters was essential in achieving reliable and interpretable classification outcomes

in the context of automatic event detection in scalp EEG data.

CML algorithms typically struggle when it comes to discovering useful patterns in very high-dimensional feature spaces. This is why dimensionality reduction techniques need to be applied to scalogram images/features before inputting them to CML algorithms for training. Principal Component Analysis (PCA) is employed for dimensionality reduction. By examining the cumulative explained variance, we determine the number of principal components needed to retain a specified amount of the original data's variance (e.g., 99%). This step reduces the number of features while preserving the most significant information, making the data more manageable and improving the efficiency and performance of the subsequent machine learning algorithms. Thus, using cumulative explained PCA, we reduce the data to the  $n$ th component, where  $n$  is chosen based on the desired explained variance threshold (99%) as illustrated in Figure 4.

The use of SVMs, Decision Trees, and Random Forest classifiers ensures a balanced approach between precision in high-dimensional data handling, interpretability, and robustness against over-fitting, all of which are essential for effectively analyzing and understanding the nuanced patterns within EEG segments.

### E. DEEP LEARNING ALGORITHMS

Deep convolutional neural networks (DCNNs) have emerged as the predominant algorithms for image and video recog-



nition tasks over the past decade, outperforming traditional machine learning methods such as support vector machines (SVMs) and random forest (RF) classifiers. Unlike conventional machine learning algorithms, which rely heavily on manual feature engineering and domain-specific knowledge, DCNNs are data-driven and adept at autonomously learning discriminative features from the input data. This inherent capability renders them more adaptable and less dependent on domain expertise, making them a versatile choice across various applications. In our research, we utilized the VGG16 [19], EfficientNetB1 [21], and GoogLeNet [20] architectures to explore their effectiveness in event localization tasks.

### 1) VGG16

The VGG16 architecture, renowned for its deep structure utilizing small  $3 \times 3$  convolutional filters, has been effectively adapted for EEG classification tasks [19]. In this study, the pre-trained VGG16 model was fine-tuned by removing its final classification layer and adding a dense layer with softmax activation to classify EEG data into three classes. The model processes input images resized to  $224 \times 224$  pixels through a series of convolutional layers, starting with 64 filters and progressively increasing to 512 filters in the deeper layers, with max-pooling applied to downsample the feature maps. Fully connected layers with 4096 units follow the convolutional layers, incorporating ReLU activation for non-linearity. Class weights were computed to address class imbalance, ensuring the model's performance across all classes. The model was trained using the Adam optimizer with a learning rate of 0.0001 and categorical cross-entropy as the loss function, using batch sizes of 32 for training and 16 for validation and testing. This fine-tuning approach harnesses VGG16's robust feature extraction capabilities while adapting it for efficient and accurate EEG data classification. EEG signals often contain intricate temporal patterns crucial for accurate classification. VGG16's depth allows it to capture both low-level and high-level temporal features, making it suitable for capturing the complex dynamics of EEG data. Additionally, the use of small convolutional filters aids in extracting fine-grained features from the EEG signals, further enhancing classification performance.

### 2) GoogLeNet

GoogLeNet, also known as Inception-v1, is recognized for its computational efficiency and innovative use of inception modules [20], making it well-suited for EEG classification tasks. This architecture, composed of 22 layers and approximately 6.7 million parameters, begins with an input layer of size  $224 \times 224 \times 3$ , followed by several convolutional layers with ReLU activation, including an initial 64-filter layer with a  $7 \times 7$  kernel and a subsequent 192-filter layer with a  $3 \times 3$  kernel. The model incorporates max-pooling layers for dimensionality reduction and further complexity management. The core of GoogLeNet is its series of inception modules, which combine  $1 \times 1$ ,  $3 \times 3$ , and  $5 \times 5$  convolutions along with max-pooling, enabling the model to efficiently process and

capture features at multiple scales from the EEG data. Additionally, two auxiliary networks are integrated after certain inception modules to assist in gradient flow during training, each consisting of an average pooling layer, a convolutional layer, dense layers, and dropout with a 0.7 rate, culminating in softmax output layers for classification. The model concludes with a global average pooling layer and a dropout layer at a 0.4 rate before the final softmax output. This design allows GoogLeNet to handle the high-dimensional and temporally dynamic nature of EEG data effectively, striking a balance between computational efficiency and the ability to capture relevant neural features, making it highly effective for classifying complex EEG signals.

### 3) EfficientNetB1

EfficientNetB1, part of a family of models known for their balanced scaling of network width, depth, and resolution, has been effectively adapted for EEG abnormality classification tasks. In this study, EfficientNetB1 was employed, consisting of 7 blocks and approximately 5.3 million parameters, to classify EEG data into three classes. The model was fine-tuned with an input layer of  $224 \times 224 \times 3$ , followed by an initial convolutional layer with 32 filters, a  $3 \times 3 \times 3$  kernel, and ReLU activation. The architecture includes MBConv blocks, which are Mobile Inverted Bottleneck Convolution blocks with varying filter sizes and expansion factors, combined with reduction and pooling layers for dimensionality reduction. A global average pooling layer and a dropout rate of 20% precede the final dense layer with softmax activation for classification. The model was trained using a batch size of 32 for the training data and 16 for the validation and test data. Class weights were computed to address class imbalance, ensuring balanced performance across all classes. The model was compiled with the Adam optimizer at a learning rate of 0.0001, using categorical cross-entropy as the loss function. This configuration strikes an optimal balance between model complexity and efficiency, enabling EfficientNetB1 to achieve high classification accuracy with fewer computational resources compared to larger architectures, making it particularly suitable for EEG abnormality detection and diagnosis in clinical settings.

By contextualizing VGG16, GoogLeNet and EfficientNetB1 within EEG classification, researchers gain insights into the unique advantages and considerations associated with each architecture. This nuanced understanding aids in selecting the most suitable model for specific EEG datasets and applications, ultimately advancing the field of EEG-based analysis and diagnosis. Our training regimen for all three models included early stopping to prevent over-fitting, utilizing the categorical cross-entropy loss function for optimization. Training spanned 30 epochs, with early stopping enforced at the 12th epoch. The Adam optimizer, coupled with a learning rate of 0.0001 determined heuristically, facilitated efficient model parameter tuning. Performance evaluation involved

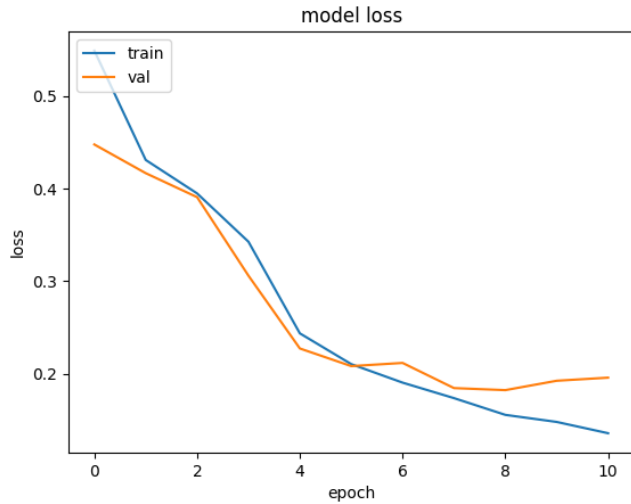


FIGURE 5. Training and validation loss curves for the VGG16 model using Morlet Wavelet on the EEG dataset.

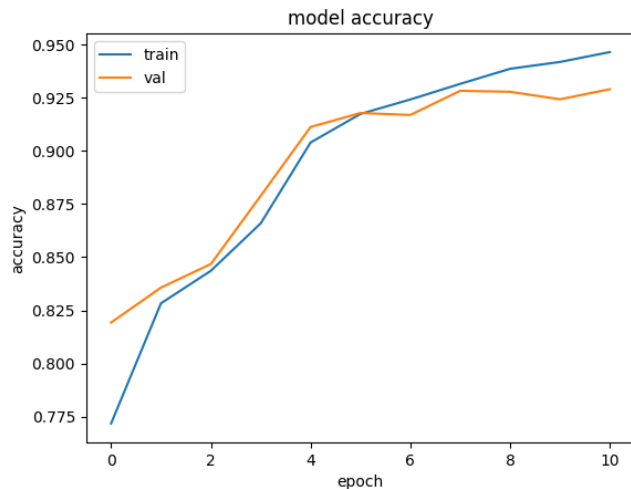


FIGURE 6. Training and validation accuracy curves for the VGG16 model using Morlet Wavelet on the EEG dataset.

monitoring loss function and accuracy metrics across epochs, as illustrated in Figure 5 and Figure 6. These comprehensive analyses provided insights into the comparative strengths and weaknesses of the architectures, guiding informed decision-making regarding their suitability for specific image and video recognition tasks.

#### IV. RESULTS AND DISCUSSION

Table 3 presents the performance evaluation metrics for six different classifiers—Decision Tree, Random Forest, Support Vector Machine (SVM), EfficientNet, GoogleNet, and VGG16—across four wavelet transform types: Mexh/Ricker, Morlet, Gaussian-1, and Gaussian-2. These metrics, namely Precision (Pre), Recall (Rec), F1-score (F1), and Accuracy (Acc), are crucial for assessing the classifiers' ability to accurately localize abnormal events within EEG signals, specifically in identifying the two main classes: Slow Waves (SW)

and Spike and Sharp Waves (SSW).

In the context of EEG event localization, the ability to accurately pinpoint the temporal and spatial locations of abnormal events is critical. This is especially important in clinical settings where the precise localization of events such as Slow Waves and Spike and Sharp Waves can directly impact diagnosis and treatment planning. The results indicate that DCNN models, particularly VGG16 and GoogleNet, tend to outperform traditional CML models. Overall, VGG16 (with Morlet) achieves the highest accuracy of 0.792; however, GoogleNet achieves better accuracy (than VGG16) when used in conjunction with Mexh/Ricker, Gaussian-1 or Gaussian-2 wavelets. DCNN models achieve accuracy greater than 0.70 in all cases except one (EfficientNet with Morlet), demonstrating consistent performance that is somewhat unaffected by the choice of wavelet. CML models, in comparison, deliver lower accuracy values and their performance seems to be dependent on the wavelet choice. The random forest model (with Mexh/Ricker) delivers the highest accuracy (0.732) among the CML models. For the Mexh/Ricker and Gaussian-1 wavelets, all three CML models obtain accuracy values greater than 0.70, whereas for Morlet and Gaussian-2 the accuracy values for the majority of CML models are less than 0.70.

The confusion matrix for VGG16 using the Morlet wavelet, shown in Figure 7, illustrates the model's ability to correctly classify EEG events into the correct categories. VGG16 shows a strong performance in distinguishing between Normal, Slow Waves, and Spike and Sharp Waves, with relatively few misclassifications. This capability is crucial in reducing false positives and negatives in a clinical setting, ensuring more reliable diagnosis. The loss and accuracy curves for the VGG16 model, presented in Figures 5 and 6, demonstrate the model's training procedure. The training and validation loss decrease steadily over epochs, indicating that the model is learning effectively without overfitting. The slight plateau observed in later epochs suggests that the model has reached a point of optimization, maintaining a balance between generalization and performance.

Additionally, the standard deviation of classification accuracy for different classifiers across multiple EEG segments depicted in Figure 8 was computed by executing the classification process multiple times for each classifier. Specifically, each classifier was trained and tested across 7 random data splits or training runs, and the accuracy was recorded for each run. The standard deviation was then calculated from these accuracy values to capture the variability in performance. VGG16, along with EfficientNet and GoogleNet, exhibits not only decent accuracy but also lower variability in predictions, as shown by their tight standard deviation intervals. This low standard deviation underscores the stability and reliability of these models across different EEG segments, making them particularly well-suited for clinical applications where consistency is paramount. Some sample results on real EEG data are shown in Figure 9.

Overall, the results, including metrics, confusion matri-

**TABLE 3. Comparison of performance evaluation metrics (Precision, Recall, F1-score, and Accuracy) for various classifiers applied to EEG event localization. For each type of wavelet, the accuracy of the best performing CML and DCNN model is highlighted using boldface text.**

Classifier Type	Mexh/Ricker				Morlet				Gaussian-1				Gaussian-2			
	Pre	Rec	F1	Acc	Pre	Rec	F1	Acc	Pre	Rec	F1	Acc	Pre	Rec	F1	Acc
Decision Tree	0.668	0.670	0.663	0.720	0.584	0.583	0.583	<b>0.654</b>	0.666	0.666	0.653	<b>0.726</b>	0.586	0.593	0.587	0.668
Random Forest	0.675	0.678	0.667	<b>0.732</b>	0.547	0.550	0.547	0.632	0.651	0.656	0.646	0.714	0.653	0.656	0.646	<b>0.716</b>
SVM	0.605	0.564	0.573	0.708	0.483	0.424	0.423	0.653	0.590	0.553	0.563	0.704	0.552	0.499	0.495	0.675
EfficientNet	0.719	0.707	0.699	0.745	0.635	0.631	0.631	0.684	0.725	0.729	0.724	0.754	0.720	0.712	0.711	0.750
GoogleNet	0.751	0.744	0.745	<b>0.778</b>	0.689	0.683	0.685	0.737	0.756	0.745	0.742	<b>0.780</b>	0.741	0.729	0.733	<b>0.767</b>
VGG16	0.722	0.712	0.714	0.751	0.754	0.751	0.746	<b>0.792</b>	0.719	0.713	0.713	0.750	0.701	0.683	0.686	0.730

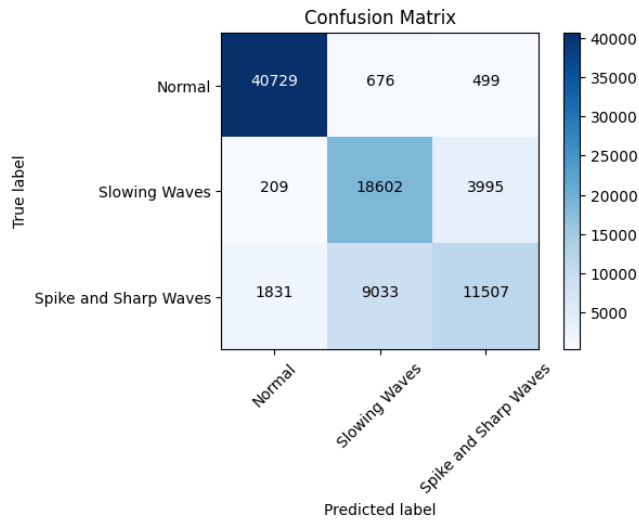


**FIGURE 7. Confusion matrix for the VGG16 model using Morlet Wavelet, showing classification performance across three classes: Normal, Slowing Waves (SW), and Spike and Sharp Waves (SSW).**

ces, loss curves, and standard deviation analyses, provide a comprehensive evaluation of the models' performance. The findings highlight the strong potential of deep learning models, particularly VGG16, in EEG event localization. VGG16 demonstrates superior accuracy, low variability, and effective training, making it well-suited for clinical applications and further research. As EEG analysis becomes increasingly important, these models are poised to advance the field, particularly in developing explainable AI systems that can accurately and reliably identify abnormal events.

## V. CONCLUSION

We have presented results for detection of events within EEG recordings in a comprehensive dataset. In this dataset, two events of interest within EEG, 'Slow waves' and 'Spike and Sharp waves', are labelled with meticulous detail across time and across channels. We believe that these detailed event labels should be highly valuable to researchers who are interested in examining EEG data from an explainable (XAI) perspective. The quality of this dataset was validated

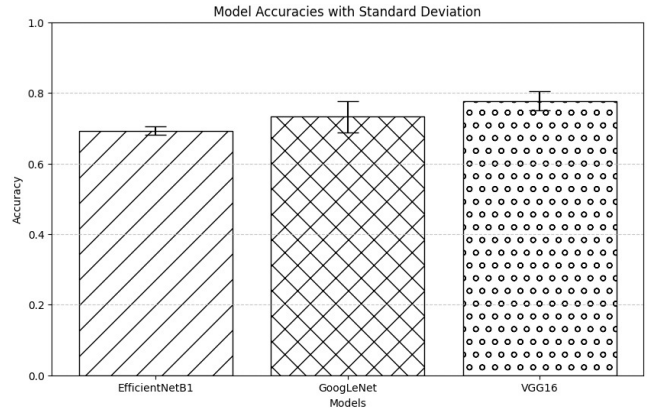


**FIGURE 8. Standard deviation of classification accuracy for different classifiers across multiple EEG segments. The classification process was executed multiple times for each classifier, with accuracy values computed for each run. The standard deviation of these accuracy values was then calculated to assess the variability in performance. The plot demonstrates the variability in performance for each classifier, VGG16 and EfficientNetB1 showing lower standard deviation, indicating more consistent and reliable predictions.**

by evaluating the performance of well-established CML and DCNN models. Overall, DCNN models outperform CML models and deliver a more consistent performance that does not degrade substantially when the classifier or wavelet models are changed. CML models in comparison are less consistent and their performance seems to be dependent on the wavelet choice; this is not unexpected given that CML model performance is known to be heavily reliant on the feature extraction front-end. Therefore, we can conclude that DCNNs deliver better performance compared to CML models on the NMT-Events dataset. However, this only applies to wavelet based features and we do not recommend generalising this conclusion to all feature categories. A decent performance was observed indicating that the learning algorithms were able to map relevant patterns to the events of interest. We believe that there is room for further improvement and development of purpose-built learning algorithms will lead to further improvement in performance. Our dataset is being made available to the public in the interest of research and our hope is that this will have a positive impact on this interesting

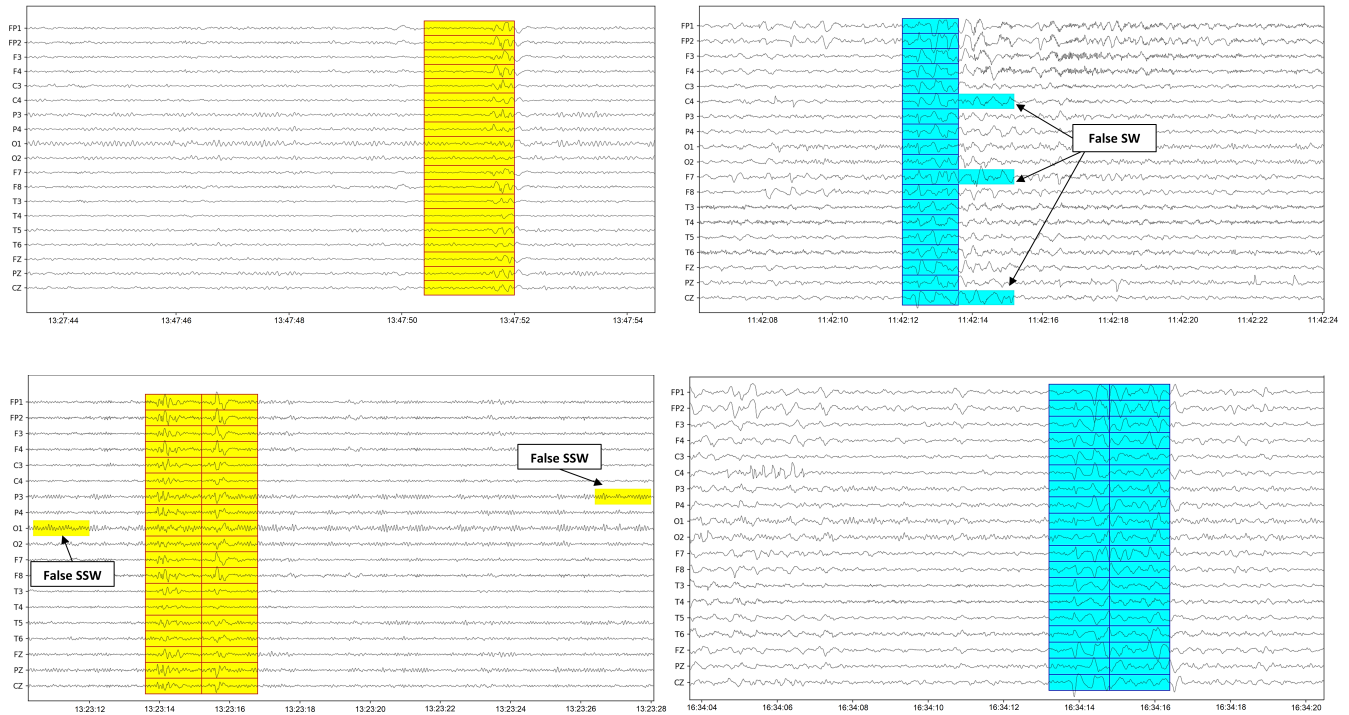


**FIGURE 9.** Some sample results demonstrating performance of the GoogLeNet based classifier on actual records. Ground-truth labels are indicated by blue bounding boxes for SW and red bounding boxes for SSW. Predictions are shown by cyan rectangles for SW and yellow rectangles for SSW. Colored rectangles not falling within any bounding box are considered false positives.

area of research. We also believe that future work on our dataset will eventually lead to development of explainability features that can augment that capability of automated EEG analysis and screening systems.

### ACKNOWLEDGMENT

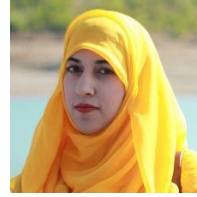
The authors are grateful to the support staff at Pak-Emirates Military Hospital, Rawalpindi Pakistan for their help in collecting data for this project. This work was funded by the University of Jeddah, Jeddah, Saudi Arabia, under grant No. (UJ-21-ICI-1). The authors, therefore, acknowledge with thanks the University of Jeddah technical and financial support.

### REFERENCES

- [1] H. A. Khan, M. A. Haider, H. A. Ansari, H. Ishaq, A. Kiyani, K. Sohail, M. Muhammad, and S. A. Khurram, "Automated feature detection in dental periapical radiographs by using deep learning," *Oral surgery, oral medicine, oral pathology and oral radiology*, vol. 131, no. 6, pp. 711–720, 2021.
- [2] I. S. Bayrakdar, K. Orhan, S. Akarsu, Ö. Çelik, S. Atasoy, A. Pekince, Y. Yasa, E. Bilgir, H. Sağlam, A. F. Aslan, and others, "Deep-learning approach for caries detection and segmentation on dental bitewing radiographs," *Oral Radiology*, pp. 468–479, 2021.
- [3] J. W. Britton, L. C. Frey, J. L. Hopp, P. Korb, M. Z. Koubeissi, W. E. Lievens, E. M. Pestana-Knight, and E. K. St Louis, *Electroencephalography (EEG): an introductory text and atlas of normal and abnormal findings in adults, children, and infants*, 2016.
- [4] WHO and the World Federation of Neurology, *ATLAS Country Resources for Neurological Disorders*, 2nd Edition, 2017.
- [5] H. A. Khan, R. U. Ain, A. M. Kamboh, H. T. Butt, S. Shafait, W. Alamgir, D. Stricker, and F. Shafait, "The NMT Scalp EEG Dataset: An Open-

- Source Annotated Dataset of Healthy and Pathological EEG Recordings for Predictive Modeling," *Frontiers in Neuroscience*, vol. 15, 2021.
- [6] S. Roy, I. Kiral-Kornek, and S. Harrer, "ChronoNet: a deep recurrent neural network for abnormal EEG identification," in *Conference on artificial intelligence in medicine in Europe*, 2019, pp. 47–56.
- [7] R. T. Schirrmester, J. T. Springenberg, L. D. J. Fiederer, M. Glasstetter, K. Eggenberger, M. Tangermann, F. Hutter, W. Burgard, and T. Ball, "Deep learning with convolutional neural networks for EEG decoding and visualization," *Human brain mapping*, vol. 38, no. 11, pp. 5391–5420, 2017.
- [8] L. A. W. Gemein, R. T. Schirrmester, P. Chrabaszcz, D. Wilson, J. Boedecker, A. Schulze-Bonhage, F. Hutter, and T. Ball, "Machine-learning-based diagnostics of EEG pathology," *NeuroImage*, vol. 220, p. 117021, 2020.
- [9] S. Mallat, *A wavelet tour of signal processing*, 1999.
- [10] M. Golmohammadi, A. H. N. Torbati, S. L. D. Diego, I. Obeid, and J. Picone, "Automatic analysis of EEGs using big data and hybrid deep learning architectures," *Frontiers in human neuroscience*, vol. 13, p. 76, 2019.
- [11] I. Ullah, M. Hussain, H. Aboalsamh, and others, "An automated system for epilepsy detection using EEG brain signals based on deep learning approach," *Expert Systems with Applications*, vol. 107, pp. 61–71, 2018.
- [12] Y. Yuan, G. Xun, K. Jia, and A. Zhang, "A novel wavelet-based model for eeg epileptic seizure detection using multi-context learning," in *2017 IEEE International Conference on Bioinformatics and Biomedicine (BIBM)*, 2017, pp. 694–699.
- [13] J. Craley, C. Jouny, E. Johnson, D. Hsu, R. Ahmed, and A. Venkataraman, "Automated seizure activity tracking and onset zone localisation from scalp EEG using deep neural networks," *PLoS one*, vol. 17, no. 2, p. e0264537, 2022.
- [14] S. Chambon, V. Thorey, P. J. Arnal, E. Mignot, and A. Gramfort, "DOSED: a deep learning approach to detect multiple sleep micro-events in EEG signal," *Journal of Neuroscience Methods*, vol. 321, pp. 64–78, 2019.
- [15] N. Bajaj, "Wavelets for EEG Analysis," in *Wavelet Theory*, 2020.
- [16] C. Cortes and V. Vapnik, "Support-vector networks," *Machine learning*, vol. 20, no. 3, pp. 273–297, 1995.

- [17] T. K. Ho, "Random decision forests," in *Proceedings of 3rd international conference on document analysis and recognition*, vol. 1, 1995, pp. 278–282.
- [18] W.-Y. Loh, "Classification and regression trees," *Wiley interdisciplinary reviews: data mining and knowledge discovery*, vol. 1, no. 1, pp. 14–23, 2011.
- [19] K. Simonyan and A. Zisserman, "Very deep convolutional networks for large-scale image recognition," *arXiv preprint arXiv:1409.1556*, 2014.
- [20] C. Szegedy, W. Liu, Y. Jia, P. Sermanet, S. Reed, D. Anguelov, D. Erhan, V. Vanhoucke, and A. Rabinovich, "Going deeper with convolutions," in *Proceedings of the IEEE conference on computer vision and pattern recognition*, 2015, pp. 1–9.
- [21] Tan, Mingxing, and Quoc V. Le. "EfficientNet: Rethinking Model Scaling for Convolutional Neural Networks," in *Proceedings of the 36th International Conference on Machine Learning, ICML*, pp. 6105-6114, 2019.
- [22] Goupillaud, P., Grossmann, A., & Morlet, J. (1984). "Cycle-octave and related transforms in seismic signal analysis," *Geoexploration*, 23(1), 85-102.
- [23] Ricker, N. (1943). "Further developments in the wavelet theory of seismogram structure," *Bulletin of the Seismological Society of America*, 33(3), 197-228.
- [24] Mallat, S. "A Wavelet Tour of Signal Processing," *Academic Press*, 1999.
- [25] Nicolaou N, Georgiou J. "Detection of epileptic electroencephalogram based on permutation entropy and support vector machines," *Expert Syst Appl*, 39(1):202-9, 2019.
- [26] Wang Y, Zhou W, Yuan Q, Li X, Meng Q, Zhao X, et al. "Comparison of ictal and interictal EEG signals using fractal features," *Int J Neural Syst*, 23(6):1350036, 2013
- [27] Ben Messaoud R, Chavez M. "Random Forest classifier for EEG-based seizure prediction," *arXiv preprint arXiv*, 2106.04510, 2021.
- [28] Rajwal, S., Aggarwal, S. "Convolutional Neural Network-Based EEG Signal Analysis: A Systematic Review," *Arch Computat Methods Eng*, 30, 3585–3615, 2023
- [29] Hastie, T., Tibshirani, R., & Friedman, J. "The Elements of Statistical Learning: Data Mining, Inference, and Prediction," *Springer*, 2009.
- [30] Faust, O., Acharya, U., Adeli, H., & Adeli, A. "Wavelet-based EEG processing for computer-aided seizure detection and epilepsy diagnosis," *Elsevier, Seizure*, 26, 56–64, 2015.
- [31] Chen, Y., Zhao, Y., Zhang, Y., & Li, J. "Advances in EEG Screening for Epileptic Seizures Using Deep Learning: A Review," *IEEE Transactions on Biomedical Engineering*, 70(3), 782-793, 2023.
- [32] Zhou, T., Zhang, L., & Yang, J. "Deep Learning Methods for Automatic EEG Classification: A Survey and Future Directions," *Frontiers in Neuroscience*, 16, 758154, 2022.
- [33] Kim, H., Lee, S., & Park, C. "Enhanced EEG Screening Techniques: A Comparative Study of Machine Learning and Deep Learning Approaches," *Neurocomputing*, 545, 398-410, 2024.
- [34] Liu, X., Xu, Y., & Zhang, Q. "Explainable AI in EEG Signal Analysis: Current Challenges and Future Directions," *Artificial Intelligence Review*, 56(2), 283-306, 2023.



**HIRA MASOOD** received her BS in Software Engineering from the International Islamic University Islamabad (IIUI), Islamabad, Pakistan in 2014 and her MS in Information Technology from the National University of Sciences and Technology, Islamabad, Pakistan in 2018. She has been working as a Research Associate at TUKL-NUST R&D Centre since September 2018.



**ADIL JOWAD QURESHI** received the B.Sc. degree in Electrical Engineering from the National University of Sciences and Technology, Islamabad, Pakistan, in 2022. From 2021 to 2022, he was an undergraduate researcher at Deep Learning Lab, NCAI, Islamabad, Pakistan. He is currently working at Strada Imaging as a Computer Vision Engineer. His research interests include applied deep learning and machine learning, computer vision and pattern recognition.



**MUIZ ALVI** received his B.Eng in Electrical Engineering from the National University of Sciences and Technology (NUST) in 2022. From 2021 to 2022, he worked as a research intern at TUKL Deep Learning Lab at NUST. Between 2022 and 2023, he worked as an Assistant AI Research Engineer at CureMD, Lahore. Currently he works as a developer for one of the leading AI companies in the world through a talent acquisition company, Turing.



**MOHAMMAD ALI ALQARNI** received the bachelor's degree in computer science from King Khalid University, Saudi Arabia, in 2008, the M.Sc. degree in computational science from Laurentian University, Sudbury, Canada, in 2012, and the Ph.D. degree in computer science from McMaster University, Hamilton, Canada, in 2016. He is currently an Associate Professor with the College of Computer Science and Engineering, University of Jeddah, Saudi Arabia.



**HAZIQ ARBAB** received the B.Sc. degree in Electrical Engineering from the National University of Sciences and Technology, Islamabad, Pakistan in 2022. From 2021 to 2022, he was an undergraduate researcher at Deep Learning Lab, NCAI, Islamabad Pakistan. He is currently enrolled in a master's degree in Artificial Intelligence at the University of Essex working with British Telecom on action recognition, computer vision, and mixed reality.



**HASSAN AQEEL KHAN** (S'07–M'16) obtained his Ph.D. degree in electrical engineering from Michigan State University, East Lansing, USA, in 2015, and his MSc degree in signal processing and communication from the University of Edinburgh, Scotland, UK in 2007. He is currently a Senior Lecturer at the Department of Applied Artificial Intelligence and Robotics, School of Computer Science and Digital Technologies at Aston University Birmingham, UK. Previously, he has worked

at the University of Jeddah, Saudi Arabia, and the National University of Sciences and Technology (NUST) Islamabad, Pakistan as an Assistant Professor. Hassan's research interests include biomedical signal processing, computational pathology and applications of AI and machine learning in medical imaging.



**FAISAL SHAFAIT** received the Ph.D. degree (Hons.) in computer engineering from the Technical University of Kaiserslautern (TUKL), Germany, in 2008. He is currently working as a Professor with the School of Electrical Engineering and Computer Science (SEECS), National University of Sciences and Technology (NUST), Islamabad, Pakistan. Previously, he was an Adjunct Senior Lecturer with the School of Computer Science and Software Engineering, The University of Western

Australia, Perth, Australia. He was a Senior Researcher with German Research Center for Artificial Intelligence (DFKI) and an Adjunct Lecturer with TUKL. His research interests include machine learning and pattern recognition with a special emphasis on applications in document image analysis. He has coauthored over 100 publications in international peer-reviewed conferences and journals in this area.

...



**AWAIS MEHMOOD KAMBOH** (S'06–M'11–SM'17) obtained his Ph.D. degree in electrical engineering from Michigan State University, East Lansing, USA, in 2010, and his MS degree in electrical engineering systems from University of Michigan, Ann Arbor, USA in 2006. He is currently a Professor at the School of Electrical Engineering and Computer Science (SEECS), National University of Sciences and Technology (NUST), Islamabad, Pakistan. He is the founding Dean of

the Open and Distance Learning at NUST and continues in this position. Previously, He has worked at the University of Jeddah, Saudi Arabia, the University of Oxford, UK as a visiting scholar, and at Evigia Systems Inc., Ann Arbor, USA as an ASIC Design Engineer. At NUST, Dr. Kamboh established the Neuroinformatics research lab, Pakistan's first research EEG lab. He also led the Analog Mixed Signal Integrated Circuit research group and was recipient of the best researcher award at SEECS. Prof. Kamboh is a Senior Member of the IEEE. His research interests include mixed-signal integrated-circuits, biomedical signal processing, and brain computer interfaces.



**SAIMA SHAFAIT** is a Consultant Neurologist at Fauji Foundation Hospital in Rawalpindi Pakistan. Prior to that she was a Registrar Neurology at Pak Emirates Military Hospital, Rawalpindi, Pakistan. She is fellow of college of Physicians and Surgeons, Pakistan and also a member of the Royal College of Physicians UK. She has almost 20 years experience of working in the healthcare sector in Pakistan. Her research interests include applications of AI and machine learning in Neurology.